

MODELING THE MECHANICAL INTEGRITY OF AIRFOIL PRINTED CIRCUIT HEAT EXCHANGERS

Ian Jentz, Mark Anderson

Department of Engineering Physics, University of Wisconsin-Madison
Madison, WI 53706
ijentz@wisc.edu

Xiaodong Sun

Nuclear Engineering Program, The Ohio State University
Columbus, OH 43210

ABSTRACT

Printed Circuit Heat Exchangers (PCHEs) are an integral part of supercritical carbon dioxide (s-CO₂) Brayton power cycles in advanced reactor designs. Better thermal efficiencies at higher source temperatures make the s-CO₂ Brayton cycle attractive for use with the High-Temperature Gas-cooled Reactor, the Sodium Fast Reactor, and the Fluoride-salt cooled High-temperature Reactor. In these reactor systems PCHEs would be used as Intermediate Heat Exchangers between the reactor coolant and the power cycle's s-CO₂ working fluid. PCHEs fulfill this role better than traditional shell and tube heat exchangers by being more compact and having greater heat transfer surface area per unit volume.

Novel PCHEs designs have the potential to increase heat transfer while decreasing pressure drop across the heat exchanger. Experimental work at the University of Wisconsin has identified these benefits in airfoil-fin channeled PCHEs. Greater surface area and the streamlined airfoil shape of conducting fins give the design an advantage over standard zig-zag and straight channel PCHEs. Despite better thermohydraulic performance, the structural integrity of airfoil-fin PCHEs is not yet quantified.

Validation of structural integrity of the airfoil PCHE design is necessary before its use in the nuclear industry. These heat exchangers will transfer heat between s-CO₂ and fluids such as helium, fluoride salts, and sodium. The high operating temperatures and pressures presented in coupling these disparate fluids in the compact PCHE make an investigation into structural integrity necessary.

Models are being developed at the University of Wisconsin to assess the structural integrity of airfoil-fin PCHEs. With high temperature mechanical performance data readily available for PCHE alloys, computer models of plasticity and creep are readily applicable to PCHE geometries. Results are presented for preliminary elastic and plastic models of the air-foil PCHE design that is being tested at the University of Wisconsin. The models provide failure predictions and an understanding of localized stress distributions that will drive eventual experimental efforts.

KEYWORDS

Printed Circuit Heat Exchanger
Mechanical Integrity
Stress Modeling

1. INTRODUCTION

Printed Circuit Heat Exchangers (PCHEs) are compact heat exchangers defined by their unique method of manufacture. The heat exchanger is made up of stacked plates containing chemically etched micro channels. The stack of plates is diffusion bonded under high temperature and load in a vacuum furnace, forming a solid heat exchanger. Working fluid varies from plate to plate, typically alternating between a hot and cold fluid, although multi-fluid systems are possible. Channel geometries vary greatly and are designed to the needs of the working fluid. In super critical carbon dioxide (s-CO₂) PCHEs channel geometry is chosen to enhance turbulence and hence improve the heat transfer of the gas. The airfoil-finPCHE geometry performs best for s-CO₂ as it has high heat transfer with low pressure drop.

1.1. The Airfoil-Fin PCHE

The airfoil-fin pattern is shown in Figure 1. The airfoils are described by the camber-less NACA airfoil equation, also shown in Figure 1. The pattern is described by the chord length of the airfoil, the thickness of the airfoil at its girth, the lateral pitch between airfoil columns (perpendicular to flow), and the axial pitch between airfoil rows (in the direction of flow). In sizing the array, chord length and axial pitch are set so that the most uniform hydraulic diameter is achieved, which occurs when the ratio of axial pitch to chord length (s/c) is 0.86 [2]. The airfoil-fin PCHE has set geometric parameters, which are given in Table I. These values were set in previous experimental analysis at the University of Wisconsin and result in a pattern that achieves 17.8% coverage of the etched PCHE plate. The etching process limits the depth of the air-foil fin channel to 1 mm, thus any increase in hydraulic diameter requires an increase in the pattern's spacing.

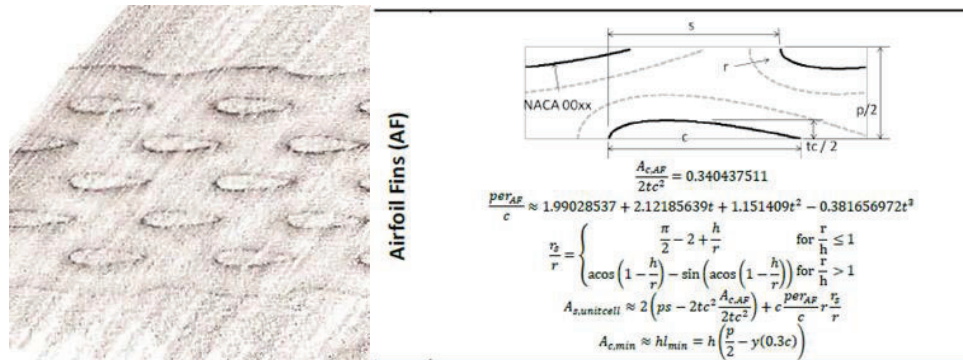


Figure 1. (left) rubbing of airfoil-fin channel, (right) camber-less NACA airfoil equation and airfoil-fin pattern [1]

Table I. Airfoil Pattern Geometry [1]

Description	Symbol	Unit	Design Value
Chord length	c	mm	4.0, 8.1
Thickness	tc	mm	0.8, 1.62
Axial pitch	s	mm	3.5, 6.9
Lateral pitch	p	mm	3.6, 7.3
Fillet radius	r	mm	0.95, 0.95
Channel depth	d	mm	0.95, 0.95
Hydraulic Diameter	D _h	mm	1.205, 1.447

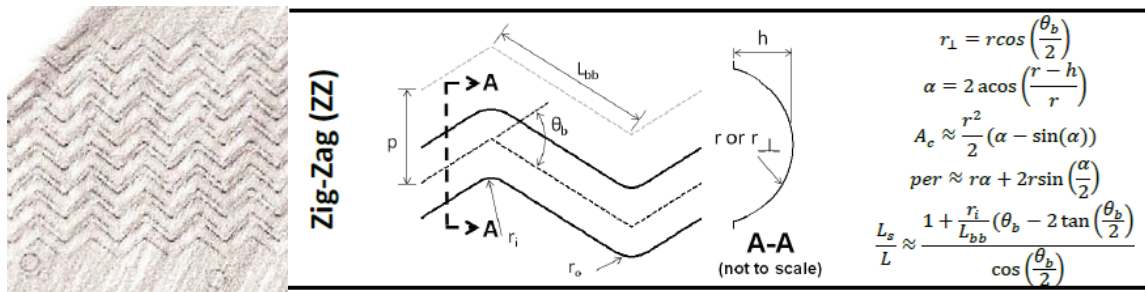


Figure 2. (left) rubbing of zig-zag channel, (right) zig-zag channel equations [1]

Table II. Zig-Zag Geometry [1]

Description	Symbol	Unit	Design Value
Bend-to-bend length	L_{bb}	mm	5.334, 4.704
Bend Angle	θ_b	deg	65, 80
Inner bend radius	r_i	mm	0.796, 0.583
Outer bend radius	r_o	mm	1.062, 0.876
Lateral pitch	p	mm	2.972, 3.277
Fillet radius	r	mm	0.95, 0.95
Channel depth	d	mm	0.95, 0.95
Hydraulic Diameter	D_h	mm	1.135, 1.116

Most experimental and numerical studies on PCHEs have focused on Heatric's™ industry standard zig-zag channel [1]. The zig-zag channel consists of many bending micro channels, as shown in Figure 2. Bends varying from 65° to 80° improve mixing of the s-CO₂ which breaks up the near wall boundary layer and enhances heat transfer. Many subsequent bends lead to high pressure loss in zig-zag channel PCHEs. Zig-zag geometry used previously at the University of Wisconsin is shown in Table II.

The airfoil-fin PCHE features a unique islanded geometry differing from most PCHE channel designs. The channels of the airfoil-fin PCHE contain an array of offset airfoil shaped fins. The fins are patterned in alternating rows with the airfoils facing the direction of flow in the channel. In this fashion, flow through the channel isn't constrained to a singular flow path as it is in typical straight and zig-zag channel designs. With the airfoil-fin design, flow is free to pass through the entirety of the airfoil array without constraint. In contrast flow channels of straight and zig-zag designs are segmented by continuous channel walls which prevent mixing of the various streams. Flow in the airfoil-fin channel is well mixed with neighboring streams, merging and separating at each subsequent airfoil-fin. This mixing allows the airfoil-fin PCHE to transfer heat as well as the standard zig-zag channel design without as much of a pressure drop. [1]

1.2. Thermodynamic Comparison of PCHE Designs

PCHE designs have been tested using s-CO₂ at the University of Wisconsin [1,2]. The system consisted of a single etched s-CO₂ flow channel. Heat flux across the channel walls was determined through measurements of the heat removed by each of 20 cooling blocks that distributed the chilled water along both ends of the flow channel. Pressure differential was measured at the inlet and outlet of the channel.

Channels investigated were two zig-zag/wavy style channels and two patterned airfoil channels, as well as a traditional straight channel design. Zig-zag channels tested featured 65° and 80° bends and are described in Table II. Airfoil channels consisted of 4.0 mm and 8.1 mm long NACA0020 airfoils and are described in Table I. Flow through all geometries covered a range of temperatures from approximately 25 to 100°C, pressures of 7.5 to 8.1 MPa, and mass fluxes of 326 to 762 kg/m²-s.

The airfoil's heat transfer performance was found to be comparable to that of the zigzag channel while achieving lower pressure losses. This can be seen in Figure 3 where airfoil channel data, represented in two cases as diamonds and hexagons, is compared to zig-zag channel data, circles and squares, as well as straight channel data, triangles. Comparing Nusselt number, the airfoil channels perform similarly to that of the zig-zag channels while besting the straight channels. The jump in Nusselt number occurs as s-CO₂ temperature crosses the pseudo-critical point. Better hydraulic performance can be noted by the airfoil channel's low Fanning friction factor in comparison to that of the zig-zag channels.

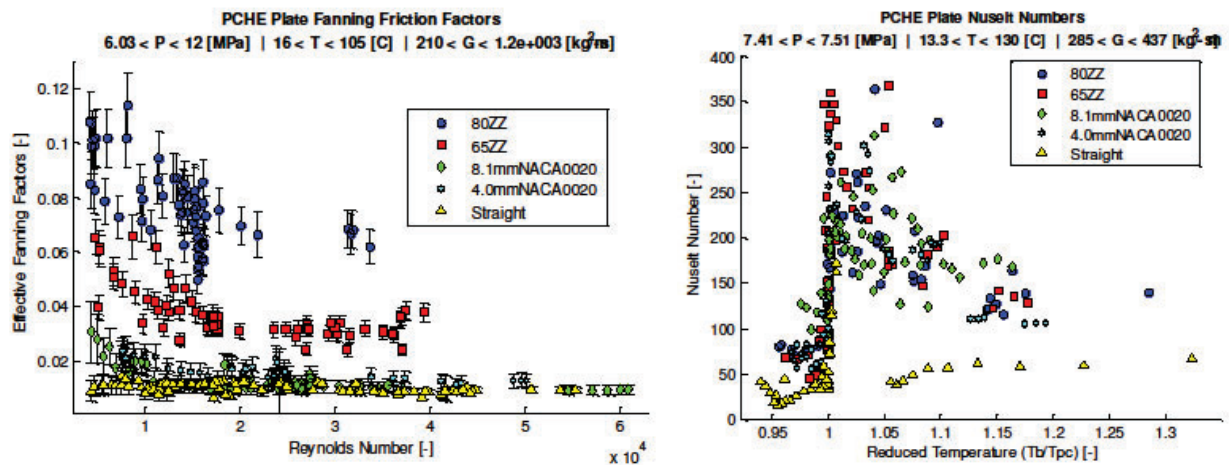


Figure 3. Performance of various flow channel geometries investigated at the University of Wisconsin. Fanning friction factors are compared for zig-zag, airfoil, and straight channels (left). Nusselt numbers were investigated about the pseudo-critical point of s-CO₂ for zig-zag, airfoil, and straight channels (right). [1]

2. MODELING MECHANICAL INTEGRITY OF THE AIRFOIL-FIN PCHE

Mechanically the airfoil-fin PCHE presents a unique problem in the evaluation of its strength. Unlike straight and zig-zag PCHE designs which use some form of continuous walled micro-channels, the airfoil-fin design has discontinuous support in the PCHE section. This support pattern creates unique stress distributions in the section that are three dimensional in their distribution, and must be modeled and understood as such. There is a great deal more complexity than is present in the stress distributions of straight and zig-zag micro-channels, which are generally two dimensional. Additional complexity results from the consideration of the entirety of a heat exchanger, including supporting exterior walls and manifold structures.

Particular concern arises with the integrity of the diffusion bond. The PCHE's stress concentrating features coincide with the diffusion bond interface. As such the fabrication of the PCHE is ultimately as important as channel geometry and loading.

2.1. Fabrication and Diffusion-Bonding Considerations

To obtain a full PCHE block, etched plates for the hot and cold side of flow are alternately stacked and diffusion bonded together, resulting in a solid heat exchanger. In the diffusion bonding process the plates are placed under load at elevated temperatures within an inert atmosphere or vacuum. This is accomplished in specialized vacuum furnaces. Loads are less than the yield strength of the parent material and temperatures are typically 50-80% that of the material melting point. Duration of loading and heating are varied to achieve the strongest bond.

At plate boundaries the applied load causes plastic deformation of the surface asperities reducing interfacial voids. Bonding then continues by diffusion controlled mechanisms including grain boundary diffusion and creep. A strong diffusion bond is formed when grains grow across the boundary, with grains ideally tripling in size. Bonds strengths 85-95% that of the base metal are achievable with sufficient grain growth [5].

Diffusion bond strength is of great concern in designing PCHEs for thermal shock testing. The success or failure of diffusion bonding is primarily governed by three bonding variables, namely, the bonding temperature, the bonding pressure, and the holding time. Furthermore, the bonding surfaces should have a good surface finish and be clean and free from oxide films and adsorbed grease.

Simple alloys, such as 316 stainless steel, diffusion bond well, with strengths 85-95% that of the base metal. PCHEs bonded out of these simple alloys are also proven to take thermal shock and fatigue well. The 316 PCHE of Pra et al. [3] withstood 100 cycles of rapid heating to 510°C and cooling to 180°C. Through all runs, helium leak testing of the fatigued PCHE didn't find any leaks.

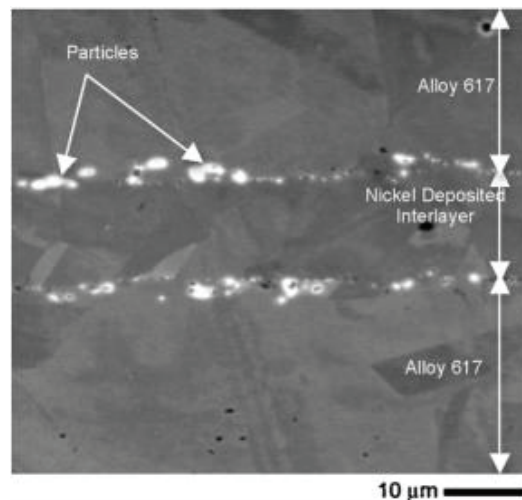


Figure 4. SEM micrograph of diffusion bonded IN617 plates featuring pure Ni interlayer. Second phase particle bound the Ni interlayer. From [5]

High temperature alloys desired for use with the HTGR do not diffusion bond as easily. Stabilizing agents, such as Al and Ti in Inconel 617 and Nb in 347 stainless steel, form tenacious oxide layers that interfere with diffusion bonding [5]. These layers can be removed and replaced with an interlayer, but bond strength is a concern. To bond an IN617 PCHE specimen by diffusion, the Ohio State University was able to electrolytically plate a 2.5- μm -thick interlayer of pure nickel to the IN617 bonding surface. This layer eliminated the formation of oxide layers prior to diffusion bonding. A scanning electron micrograph of the diffusion bond can be seen in Figure 4. Although allowing IN617 to be diffusion bonded, the nickel interlayer presented a weakened bond. The interlayer which inhibited grain growth

was a weaker material, and brought many inclusions from the plating process into the diffusion bond. Tensile and creep tests found a bond with a ~30% reduction in ultimate tensile strength, with failures occurring at the nickel interlayer. [4]

2.2. Modeling of Mechanical Integrity

Modeling of mechanical stress in the airfoil PCHE considers the complexities of geometry, material, and stress models used. Models were developed starting from the simplest geometries with the most basic material properties and stress model assumptions. With simple model results the modeling effort complexity was increased and continues to be increased. Geometries, materials, and stress models are discussed briefly before discussion of particular modeling cases.

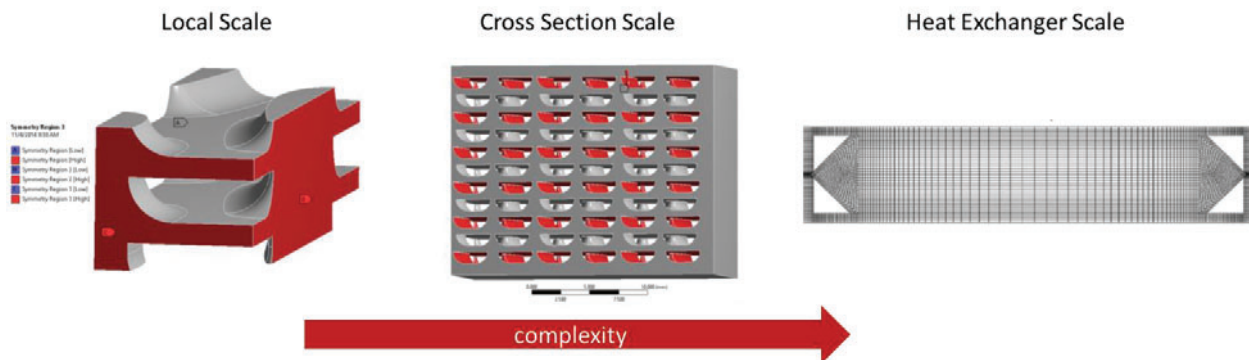


Figure 5. Geometry scales of the model effort with the local scale being the simplest model and the full heat exchanger scale being the most difficult to model

The geometry of the airfoil PCHE structure is split between three different scales, the local scale, the cross section scale, and the full heat exchanger scale. Illustrations of the three scales are shown in figure 5. The local scale is geometry immediately surrounding the airfoil channel and can be generally modeled as repeating unit cell which is inherent to the interior of the overall heat exchanger. The cross section scale encompasses geometries of the heat exchanger cross section including walls and surrounding support structures. As such, the cross section scale is considerably more complex than the local scale. The full heat exchanger scale looks at the entirety of the heat exchanger including manifolding. It is the most complex and is often simplified with porous media properties drawn from the local and cross sectional scales.

The materials modeled are those that will be experimentally tested, they are 316 stainless steel and Accura 60 (a plastic resin). These were chosen as test sections and can be made of both materials. The diffusion bonding of 316 stainless steel is readily achievable at vendors such as Vacuum Process Engineering and Refrac. 316 is also substantially cheaper than nickel alloys being considered for PCHE systems. Accura 60 is a resin that is printable through Stereolithography (SLA), which is cheaper and quicker to manufacture than diffusion bonding. Most modeling uses 316 stainless steel as the PCHE material, Accura 60 is only used for models of Accura 60 pressurization tests. Choice in the material modeled drives the choice of stress model that is used. Modeling of the ductile 316 stainless steel can be carried out to the full extent to its plasticity, while a model of the brittle Accura 60 is simply elastic.

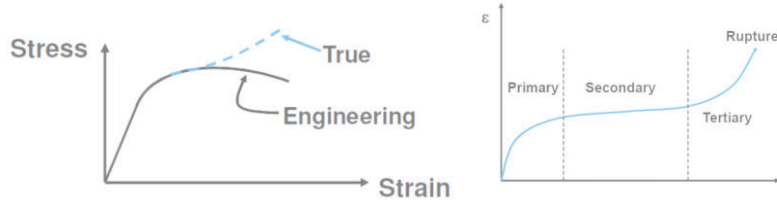


Figure 6. Stress models used in the ANSYS solver, (left) linear elastic model and its extension into the plastic model, (right) full creep model

Stress models are split between three degrees of increasing complexity, the elastic model, the plastic model, and the creep model. The elastic model is a simple linear stress-strain model with Young’s Modulus of Elasticity as the slope of the stress-strain curve. It is only valid up to the yield stress, at which point the plastic model must be used. The plastic model assumes the true stress-strain curve above the yield point is known. It is valid for any static model, if time is to be considered the creep model is used. The creep model is the most complex and must be built out of a set of plastic stress-strain models each from different length creep tests. Figure 6 depicts the stress-strain relations used in each model. The stress models available depend on the quality of material data available. A wealth of stress-strain data is available for 316 stainless steel, while properties beyond Young’s Modulus and ultimate tensile strength are not known for Accura 60.

ANSYS Mechanical and ANSYS Workbench were used in the finite element analysis (FEA) of the airfoil PCHE system. In all models the geometry of interest is transformed into a mesh of tetragonal elements which is used by the ANSYS solver. The ANSYS solver is an iterative force based solver. From the geometry and loading conditions, the forces on each element are resolved. With the forces set for each element of the geometric mesh, strain is varied and the process repeated until a solution converges. The ANSYS solver can handle all three stress models and calculates strain in the order of model complexity, from elastic, through plastic, to creep, as shown below.

$$\varepsilon = \varepsilon_{elastic} + \varepsilon_{plastic} + \varepsilon_{creep} \tag{1}$$

Plastic and elastic properties of 316 stainless steel were obtained from the ASME Boiler and Pressure Vessel Code (BPVC) [6]. Data was extracted from stress-strain charts in the BPVC’s main pressure vessel section (section III division I). The charts show experimental stress-strain data at 15 different high temperatures ranging from 427°C to 816°C with creep tests of up to 34 years performed at all temperatures. Chart data was simplified to a 9 data point fit for each temperature’s elastic stress-strain curve. Since BPVC data is only given for 15 discrete temperatures, data for intermediate temperatures was interpolated. For example stress-strain data for 316 stainless steel at 550°C was interpolated from BPVC data for 538°C and 566°C as shown in Figure 7.

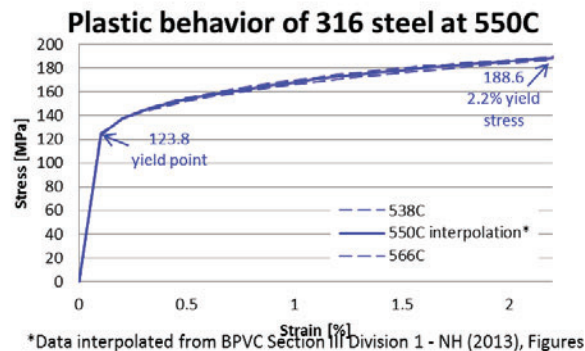


Figure 7. stress-strain data for 316 stainless steel at 550°C

3. MECHANICAL MODELING RESULTS

3.1 Elastic Models

Elastic models were the first developed because of their simplicity and usefulness in determining qualitative mechanical properties. This model is good at identifying stress concentration of the geometry and the effect of boundary conditions and supporting walls in a section. The results of the elastic models were useful in furthering of 316 stainless steel models and in predicting the onset of brittle failure in SLA printed specimens.

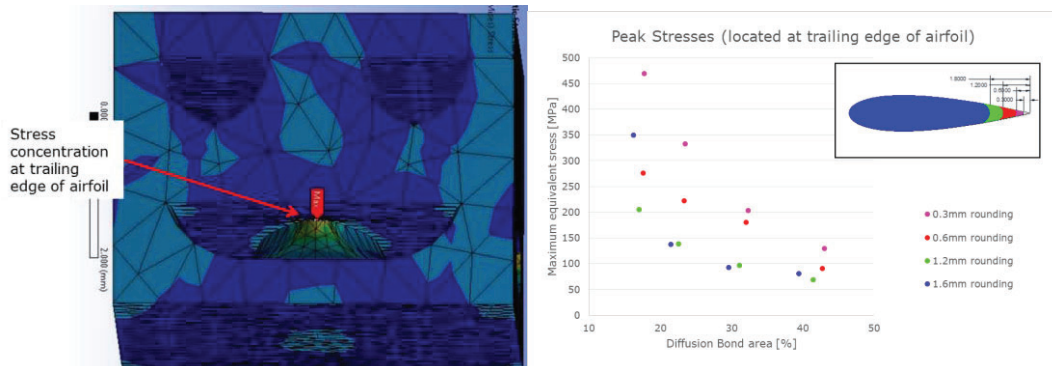


Figure 8. (left) tail side stress concentration on a local scale model. The bottom channel is pressurized while the top channel is without pressure. (right) plot of local elastic model results for stress concentration at the airfoil tail for various channel coverage and rounding of the airfoil tail

Local scale elastic modeling highlighted the head and tail of the airfoil-fin as the area of concern for airfoil PCHE systems. The local scale is enforced by applying symmetry conditions to the six faces of the unit cell. In these models 20 MPa of pressurization in the airfoil channel created stress concentrations in excess of the yield point of 316 stainless steel (123.8 MPa at 550°C) [6]. Figure 8 shows the location of the tail side stress concentration in an elastic model. Here the lower airfoil channel is pressurized while the upper straight channels are not pressurized. Large curvature at the head and tail combine with the diffusion bond interface to create a high localized concentration of stress.

Increasing the coverage of airfoils in the section by decreasing the lateral spacing between airfoil columns brings the stress concentration down by distributing the 20 MPa within the channel over more tightly packed airfoils. Decreasing the curvature at the tail of the airfoil by rounding its profile also decreases the stress concentration, as the geometric concentration is more spread out. This can be seen in the plot of results shown at the right in Figure 8. Here the maximum stress at the concentration is compared to the airfoil coverage for various tail rounding. The embedded picture shows the four rounding profiles, with more rounding creating less curvature at the airfoil tail.

Cross section scale elastic modeling was used to show the effect of wall structures in the PCHE cross section and to determine the onset of brittle failure in an SLA printed part. Since stress concentrations at the tail of the airfoil-fin were identified in previous models, they could be used to evaluate the variation of stress states in a cross sectional sample. The cross section of concern consists of 11 stacks of airfoil plates surrounded by exterior walls, as shown in Figure 9. The plates are 12 airfoil columns wide and feature the airfoil pattern shown in Figure 1. Symmetry is used at the center of the cross section, the left face of Figure 9 being the centerline and symmetry of the cross section while the right face is the surrounding wall. In the model the cross section is pressurized to 1 MPa at every other plate and the stress concentration is evaluated at each airfoil tail. A plot of the airfoil tail stresses over the cross section is

shown on the right side of Figure 9 with circular points representing the location of each airfoil tail. The airfoil tails next to the PCHE wall, on the right side of the model, exhibit the least stress as they are substantially supported by the adjacent wall. This support diminishes quickly when moving away from the wall. It was found that all but the airfoils nearest to the wall see the impact of the wall's support and thus are stressed similarly. Higher stresses occurred in the pressurized channels than those without pressurization. This inter-channel stress difference can be seen in the horizontal striation of Figure 9.

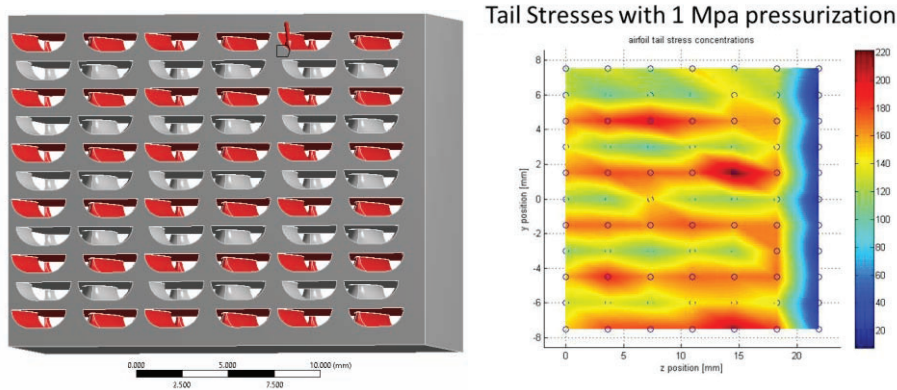


Figure 9. (left) elastic cross-section model featuring 11 stacked airfoil channels and supporting PCHE walls. Red channels are pressurized. Symmetry about left face is used to get a full cross section. (right) airfoil tail stress results for the elastic cross section model. Airfoils near wall have lower stress due to wall support. Pressurized channels have highest stresses.

These cross section results are useful in predicting the onset of brittle failure in the identical SLA printed piece. Made out of Accura 60, the SLA printed section has an ultimate tensile strength of 58 MPa. The 1 MPa pressurization model results shown in Figure 9 have a maximum stress of 222 MPa. Since the model and material are elastic, this result can be linearly extrapolated to find that a 262 kPa pressurization would yield the 58 MPa ultimate tensile strength of the part. Thus brittle failure of the SLA printed part is expected to begin at a pressurization of 262 kPa.

3.2 Plastic Models

Plastic models were used to extend the simulation effort past that of previous elastic models. In PCHEs constructed of 316 stainless steel or other ductile metal the stress concentration seen in elastic models should yield away to some extent. As the stress concentration passes the yield point, the material should strain away. This should alter the geometry to an extent and allow the stress to spread out within the yielding section. Yielding is allowable to some extent, as small features that contain stress concentrations make up a minuscule portion of the overall supporting structure. The airfoil PCHE structure should be able to withstand pressurization far above that which initiates the onset of yielding.

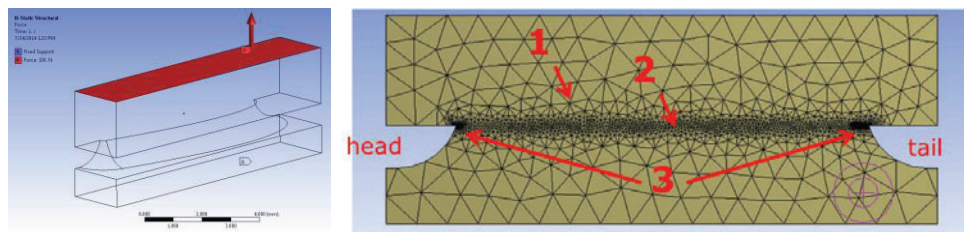


Figure 10. Plastic model of airfoil in tension. (left) tensile loading, (right) refinement of the model mesh with course mesh in channel was (1) refined mesh at the diffusion bond interface (2) and further refinement at the head and tail (3)

A local plastic model was developed to investigate the propagation of yielding in a singular airfoil-fin. The model is shown in Figure 10 and consists of a single air-foil fin under a tensile load. Tensile loading is the primary form of loading in the pressurized airfoil PCHE system. The model contains a geometric mesh with refinement of the mesh size at the diffusion bond interface and further refinement at the head and tail of the airfoil fin. The area of interest with respect to yielding is the diffusion bond interface, as it is the weakest part in the PCHE assembly and also the area of highest stress.

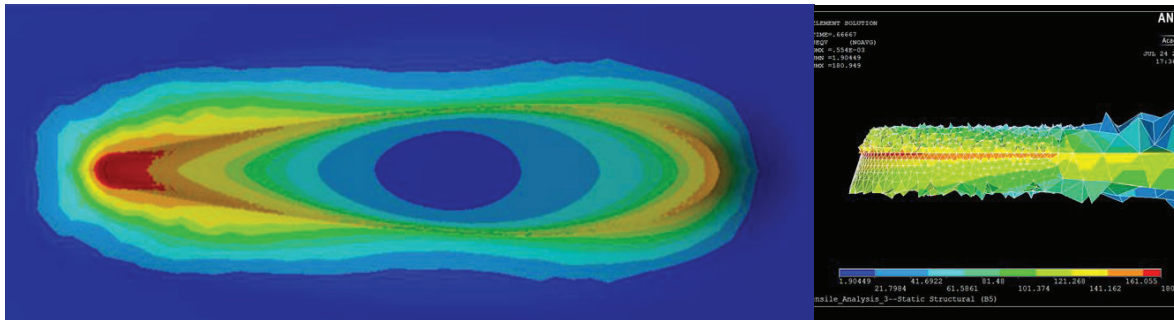


Figure 11. Propagation of yielding at the diffusion bond interface. (left) yielding propagates from head and tail of airfoil diffusion bond, (right) close up of yielding at the tail of diffusion bond

Solving the plastic airfoil-fin tensile model for various tensile loads shows the propagation of yielding in the airfoil. Figure 11 shows the distribution of stress along the diffusion bond interface with the areas of highest stress (in red) propagating through yielding from the head and tail of the airfoil. A 0.2mm thin area around the diffusion bond was analyzed to determine the extent of yielding. The percent of diffusion bond yielded was taken as the percent of this thin volume that was in excess of the 316 stainless steel yield stress of 123.8 MPa at 550°C. The airfoil can hold loads up to 1200 N at 550°C with the diffusion bond yielding no more than 20%. A plot of yielding with tensile load and a plot of yielding as a function of airfoil coverage at 20 MPa pressurization can be seen in Figure 12.

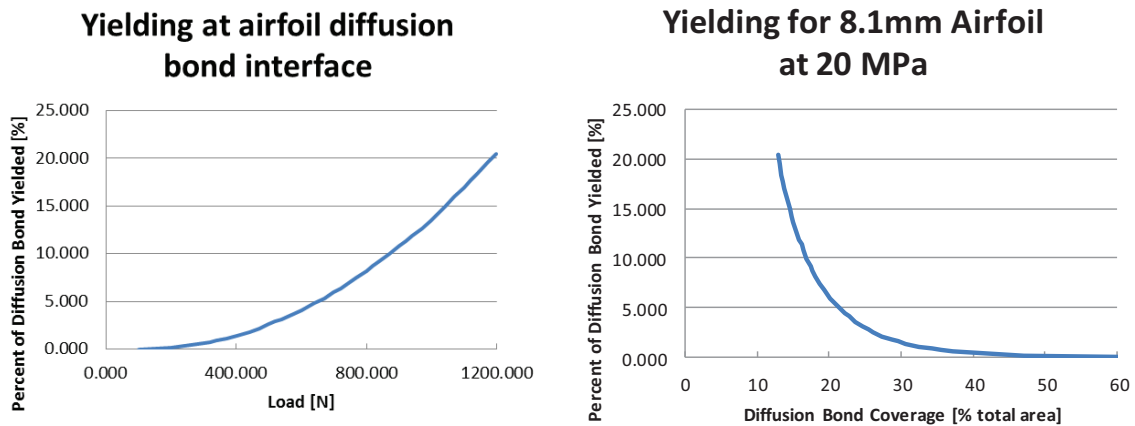


Figure 12. Percent yield of the diffusion bond interface, (left) in terms of load on a single airfoil, (right) in terms of airfoil bond coverage with pressurization of 20 MPa

These plastic models will be expanded in the future to encompass a full cross section model. This will be used to predict the failure of a full 316 stainless steel PCHE section.

CONCLUSION

Finite element analysis (FEA) models were developed to assess the structural integrity of airfoil-fin PCHEs. Airfoil-fin geometries were modeled because they achieve better thermohydraulic performance than other leading PCHE designs but have not had their mechanical strength verified. To properly model the airfoil-fin PCHE, plastic properties of 316 stainless steel were adapted for use within ANSYS Mechanical's iterative force based FEA solver. Although stress concentrating geometries reached the yield point of 316 stainless steel at channel pressurizations below 20 MPa, airfoil-fin strength is maintained with further loading due to the dispersion of the yielding stress concentration. Total yielding of the airfoil-fin's diffusion bond was found to be below 20% at 20 MPa of channel pressurization if adequate air-foil coverage of 13% or more is maintained. Pressurized air-foil fin PCHE channels can be kept safe from total plastic failure by ensuring adequate airfoil-fin coverages or 13% of the bond surface or more.

ACKNOWLEDGMENTS

Work at the University of Wisconsin-Madison and the Ohio State University is supported by the U.S. Department of Energy's Nuclear Energy University Programs.

REFERENCES

1. M. Carlson, "Measurement and Analysis of the Thermal and Hydraulic Performance of Several Printed Circuit Heat Exchanger Channel Geometries," *M.S. Thesis*, University of Wisconsin Madison, (2012).
2. A. M. Kruijenga, "Heat Transfer and Pressure Drop Measurements in Prototypic Heat Exchangers for the Supercritical Carbon Dioxide Brayton Power Cycles," Madison, 2010.
3. F. Pra, P. Tochon, C. Mauget, J. Fokkens, S. Willemsen, "Promising Designs Of Compact Heat Exchangers For Modular HTRs Using The Brayton Cycle," *Nuclear Engineering and Design*, 238, 11, 3160, (2008).
4. S. Mylavarapu, X. Sun, R. Christensen, R. Unocic, R. Glosup, M. Patterson, "Fabrication And Design Aspects Of High-Temperature Compact Diffusion Bonded Heat Exchangers," *Nuclear Engineering and Design*, 249, 49-56, 49, (2014).
5. Personal conversation with Norm Hubele of Refrac Systems, June 9, 2014.
6. ASME BPV Code, section III Division 1 - NH, (2013)